Consistency tests of ΛCDM from the early integrated Sachs-Wolfe effect: Implications for early-time new physics and the Hubble tension

Sunny Vagnozzi[*]
Kavli Institute for Cosmology (KICC) and Institute of Astronomy, University of Cambridge, Madingley Road, Cambridge CB3 0HA, United Kingdom

(Received 15 June 2021; accepted 22 July 2021; published 15 September 2021)

New physics increasing the expansion rate just prior to recombination is among the least unlikely solutions to the Hubble tension and would be expected to leave an important signature in the early integrated Sachs-Wolfe (eISW) effect, a source of cosmic microwave background (CMB) anisotropies arising from the time variation of gravitational potentials when the Universe was not completely matter dominated. Why, then, is there no clear evidence for new physics from the CMB alone, and why does the Λ cold dark matter (ΛCDM) model fit CMB data so well? These questions and the vastness of the Hubble tension theory model space provide the motivation for general consistency tests of ΛCDM. I perform an eISW-based consistency test of ΛCDM introducing the parameter $A_{\rm eISW}$, which rescales the eISW contribution to the CMB power spectra. A fit to *Planck* CMB data yields $A_{\rm eISW} = 0.988 \pm 0.027$, in perfect agreement with the ΛCDM expectation $A_{\rm eISW} = 1$ and posing an important challenge for early-time new physics, which I illustrate in a case study focused on early dark energy (EDE). I explicitly show that the increase in ω_c needed for EDE to preserve the fit to the CMB, which has been argued to worsen the fit to weak lensing and galaxy clustering measurements, is specifically required to lower the amplitude of the eISW effect, which would otherwise exceed ΛCDM's prediction by ≈20%: this is a generic problem beyond EDE that likely applies to most models enhancing the expansion rate around recombination. Early-time new physics models invoked to address the Hubble tension are therefore faced with the significant challenge of making a similar prediction to ΛCDM for the eISW effect while not degrading the fit to other measurements in doing so.

DOI: 10.1103/PhysRevD.104.063524

I. INTRODUCTION

The six-parameter Λ cold dark matter (ΛCDM) model has proven to be extremely successful in explaining a wide range of cosmological and astrophysical observations, including observations of the cosmic microwave background (CMB), the clustering of the large-scale structure (LSS), the magnitude-redshift relation of distant type Ia supernovae (SNeIa), and light element abundances [1–10]. However, discrepancies between independent inferences of cosmological parameters under the assumption of ΛCDM might be a sign of the model's incompleteness and pave the way toward new physics: this should not come as a surprise, given that several of the ingredients of ΛCDM, not least the nature of the dark sector, remain puzzling to date [11–13]. Among these discrepancies, the most significant one is the "Hubble tension," which refers to a persisting mismatch between several early- and late-time inferences of the Hubble constant H_0 [14–16].

The possibility that the Hubble tension calls for new physics is being given very serious consideration in the literature (see, e.g., Refs. [17–94]). This new physics should be able to accommodate a higher value of H_0 from CMB data while complying with constraints from other datasets: examples are baryon acoustic oscillations (BAOs) [8,95,96] and Hubble flow SNeIa measurements [4], which severely restrict the possibility of solving the Hubble tension via global late-time new physics. These measurements single out the least unlikely scenarios as those operating at early times, prior to and around recombination, and lowering the sound horizon at recombination by ≈7% [97–103]. However, it is fair to say that none of the many proposed new physics models have succeeded at the task of solving the Hubble tension while at the same time not degrading the fit to other datasets or worsening other discrepancies.

The theory model space with regard to the Hubble tension is extremely vast and, besides the few data-driven indications discussed above, is short of a clear direction. In this sense, two types of analyses can be very useful to either point toward a definite direction toward which to move or further restrict the set of viable directions:

[*]sunny.vagnozzi@ast.cam.ac.uk

(i) model-agnostic tests of new physics, and (ii) consistency tests of the ΛCDM model.[1] The analysis I will pursue in this paper, while by construction focused more on (ii), will contain a combination of these two features.

A non-negligible amount of early-time new physics needs to be present around the time of recombination for it to solve the Hubble tension [101]. One would therefore expect this new physics to already show up in CMB data alone, even before looking at local H_0 measurements. The key question motivating my analysis is then the following: Why is there no clear evidence for new physics from CMB data alone?, or this closely related question, Why does the ΛCDM model fit CMB data so well? While the two might at first glance sound like trivial questions, I believe that finding a clear answer to them can teach us valuable general lessons not only on why several early-time modifications to ΛCDM ultimately fail at solving the Hubble tension, but perhaps also on which direction(s) one should look toward in an attempt to construct successful early-time new physics models.

Where should a non-negligible amount of early-time new physics first show up in the CMB? The answer for many models, I argue, has to do with the early integrated Sachs-Wolfe (eISW) effect. The eISW effect is a contribution to CMB anisotropies arising from time-varying gravitational potentials at early times, immediately after recombination, when the Universe was not entirely matter dominated [106,107]. It is then not hard to understand why new physics altering the expansion rate around recombination would almost inevitably leave an important imprint on the eISW effect. In fact, one can generically expect that many types of early-time new physics models introduced to solve the Hubble tension will *enhance* the amplitude of the eISW effect.

These considerations provide the motivation for a consistency test of the ΛCDM model: to test whether its predictions for the eISW effect fit CMB data well. I perform such a consistency test by introducing the parameter $A_{\rm eISW}$, which artificially rescales the eISW contribution to the CMB power spectra. This is closely reminiscent of the better known $A_{\rm lens}$ lensing amplitude, rescaling the amplitude of lensing in the CMB power spectra [108]. Inferring a value of $A_{\rm eISW}$ that is strongly inconsistent with the standard value $A_{\rm eISW}=1$ could be a clear sign of early-time new physics in the CMB alone, whereas the converse could present an important challenge for these models.

From a fit to the *Planck* 2018 CMB temperature and polarization anisotropy measurements, I find $A_{\rm eISW}=0.988\pm0.027$, showing that ΛCDM's prediction for the amplitude of the eISW effect is in perfect agreement with the data. To illustrate the implications for early-time new physics, I provide a case study focused on the well-known early dark energy (EDE) model, one of the leading contenders to solve the Hubble tension [17–42]. EDE's success hinges upon its ability to accommodate a higher value of H_0 while fitting CMB data as well as ΛCDM. This comes at the price of an increase in the cold dark matter (DM) density ω_c, which has been argued to worsen the fit to weak lensing (WL) and galaxy clustering measurements, possibly leading to the demise of the EDE model as a solution to the Hubble tension [25,30,31] (see, however, a partial rebuttal of these results in Refs. [34,35]). I explicitly show that the increase in ω_c is required to lower the amplitude of the eISW effect, which would otherwise be overpredicted by ≈20%, well beyond what is allowed by the data.

The problems faced by EDE in the context of the eISW effect, and the required increase in ω_c, might actually more generally be a stumbling block for several other early-time new physics models proposed to solve the Hubble tension, particularly if these models enhance the expansion rate around recombination. It is in this sense that matching ΛCDM's prediction for the eISW effect presents an important challenge for early-time new physics. While not being a strict *no-go theorem*, these results place further restrictions on the possibility of solving the Hubble tension with early-time new physics alone and support recent findings along a related line [109–115].

The rest of this paper is organized as follows. In Sec. II I review the physics of the early ISW effect and discuss how $A_{\rm eISW}$ is introduced from a practical point of view, alongside the impact of this parameter on the CMB power spectrum. In Sec. III I discuss the datasets and analysis methodology that I make use of. The results of this analysis are presented in Sec. IV. The importance of these results in the context of early-time new physics is investigated through a case study focused on early dark energy in Sec. V. Finally, in Sec. VI I provide concluding remarks. I recommend that very busy readers skip to the key results presented in Table I and Fig. 2, whereas slightly less busy readers could also consult Table III and Fig. 4 if they are interested in the extended parameter space results, or Figs. 5 and 6 if they are interested in the early dark energy case study.

II. EARLY ISW EFFECT

I work in the Newtonian gauge on a spatially flat background where the perturbed line element is characterized by the two scalar potentials Ψ and Φ: the former is the Newtonian gravitational potential, i.e., the perturbation to the metric element $g_{00}=-1-2\Psi$, while the latter is the perturbation to the metric element $g_{ij}=a^2\delta_{ij}(1+2\Phi)$ (see Ref. [116] for a pedagogical discussion). I denote by $\Theta\equiv\delta T_\gamma/\bar{T}_\gamma$ the relative photon temperature shift, quantifying the deviation of the CMB photon distribution from that of a perfect blackbody, and by Θ_ℓ the ℓth multipole moment of Θ (after moving to Fourier space).

When one focuses on a given multipole ℓ, $\Theta_\ell(k)$ receives contributions from several source terms,

[1]A particularly interesting consistency test of ΛCDM is via the use of so-called metaparameters; see, e.g., Refs. [104,105].

including the gravitational redshift of CMB photons at the surface of last scattering (Sachs-Wolfe effect), Doppler shifting, and CMB polarization. The effect I will be interested in is the integrated Sachs-Wolfe (ISW) effect, a contribution to the CMB anisotropies resulting from time-varying gravitational potentials. Since gravitational potentials are constant in a matter-dominated Universe, the ISW effect can be active only (i) at early times, when potentials decay in the presence of a non-negligible radiation component, and (ii) at late times, when their decay is due to the dark energy component responsible for cosmic acceleration. The former contribution corresponds to the eISW effect, while the latter corresponds to the late ISW effect. In this paper, of the two I will be interested only in the eISW effect.

To linear order in temperature perturbations, the contribution of the eISW effect to $\Theta_\ell(k)$, which I denote by $\Theta_\ell^{\rm eISW}(k)$, is given by

$$\Theta_\ell^{\rm eISW}(k) = \int_0^{\eta_m} d\eta e^{-\tau(\eta)}[\dot{\Psi}(k,\eta) - \dot{\Phi}(k,\eta)]j_\ell(k\Delta\eta), \quad (1)$$

with η denoting conformal time, $\tau(\eta)$ the optical depth to a given conformal time, j_ℓ the spherical Bessel function of order ℓ, and $\Delta\eta \equiv \eta - \eta_0$, where η_0 is the conformal time today. Finally, η_m is the conformal time at an arbitrary point deep inside the matter-domination era (the exact value of η_m is irrelevant since gravitational potentials are constant in a matter-dominated Universe).

The eISW effect is expected to be dominant around recombination, when the contribution of radiation to the Universe's energy budget is still important. Because of this, Eq. (1) can be approximated by setting the argument of j_ℓ to $k\Delta_{\rm rec} \equiv k(\eta_{\rm rec} - \eta_0)$, with $\eta_{\rm rec}$ the conformal time at recombination. If I further make the approximation $\Psi \approx -\Phi$, valid in the absence of anisotropic stress, Eq. (1) is then well approximated by

$$\Theta_\ell^{\rm eISW}(k) \propto 2j_\ell(k\Delta_{\rm rec})[\Psi(k,\eta_m) - \Psi(k,\eta_{\rm rec})]. \quad (2)$$

From Eq. (2) one sees that the eISW effect receives contributions mainly from perturbations with wave number $k \sim 1/\eta_{\rm rec}$. Combined with the fact that the eISW effect adds in phase with the Sachs-Wolfe contribution to Θ_ℓ (as the two are multiplied by the same Bessel function), this shows that the main consequence of the eISW effect is to boost the height of the first acoustic peaks, the first one in particular.

My goal is now to isolate the eISW contribution to CMB power spectra, and to phenomenologically rescale this contribution by a factor whose value will then be determined by the data. Throughout this paper, I will refer to this factor as the "eISW amplitude" and will denote it by $A_{\rm eISW}$. To do so, I multiply the integrand of Eq. (1) by a function $f(\eta)$ which takes the value $A_{\rm eISW}$ if $z(\eta) > z_t = 30$, and 1 otherwise. The choice of $z_t = 30$ is purely phenomenological and dictated by the fact that the minimum of the ISW source term occurs roughly for $z \sim 30$. I have explicitly checked that other reasonable choices of z_t have no effect on my results, insofar as z_t is chosen to be deep within the matter-dominated era.

Note that at least three earlier works previously introduced $A_{\rm eISW}$, which was constrained using data from WMAP7 and the South Pole Telescope (SPT) [117], from the *Planck* 2015 data release [118], and finally from the *Planck* 2018 temperature data alone [119]. It is, of course, worth revisiting constraints on $A_{\rm eISW}$ not only in light of the *Planck* legacy data release (including polarization data, for reasons discussed toward the end of Sec. IV, and assessing the stability of the results against a different choice of high-ℓ *Planck* likelihood [120]), but especially with an eye toward early-time new physics models, given their potential to address the Hubble tension. Note, furthermore, that $A_{\rm eISW}$ bears close resemblance to the better known $A_{\rm lens}$, a phenomenological scaling parameter which rescales the amount of lensing in the CMB power spectra [108]. *Planck* primary CMB measurements exhibit a $\gtrsim 2\sigma$ preference for $A_{\rm lens} > 1$ [5]: this "lensing anomaly" is not supported by the amplitude of the *Planck* CMB lensing power spectrum $C_\ell^{\phi\phi}$ reconstructed from the temperature four-point function [121], or by the latest Atacama Cosmology Telescope results [7], and might be the result of a statistical fluctuation [120]. Much like $A_{\rm lens}$, $A_{\rm eISW}$ is a purely phenomenological scaling parameter: rather than as standard cosmological parameters, $A_{\rm eISW}$ and $A_{\rm lens}$ should be viewed as consistency test parameters.

In Fig. 1, I show the effect of varying $A_{\rm eISW}$ on the CMB temperature power spectrum while keeping all the other cosmological parameters fixed. Relative to the standard case $A_{\rm eISW} = 1$, from Fig. 1 one sees that the main effect of varying $A_{\rm eISW}$ is to enhance (suppress) power for $A_{\rm eISW} > 1$ ($A_{\rm eISW} < 1$), with the change in power being most evident for the first peak, as I anticipated earlier from Eq. (2). This is clear from the bottom panel of Fig. 1, which shows that the largest relative enhancement/suppression of power occurs at multipoles $\ell \sim 100$, i.e., around the first peak. Varying $A_{\rm eISW}$ also has a subdominant effect on the higher acoustic peaks.

In the rest of this paper, rather than fixing $A_{\rm eISW}$ to the standard value $A_{\rm eISW} = 1$, I will allow the eISW amplitude to vary and let the data constrain this parameter, first within a seven-parameter $\Lambda{\rm CDM} + A_{\rm eISW}$ model, then within extensions thereof. This will serve as an important consistency test of ΛCDM. Inferring a value of $A_{\rm eISW}$ consistent with 1 would indicate that the ΛCDM prediction for the eISW effect fits the *Planck* data remarkably well, which in turn could pose a challenge for early-time new physics. Conversely, any deviation from $A_{\rm eISW} = 1$ could provide clues as to where and what kinds of early-time modifications are necessary or even allowed. This consistency test

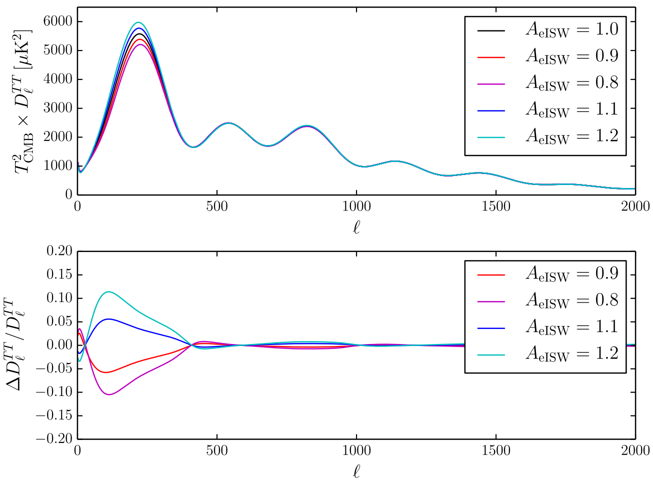

FIG. 1. Impact of varying $A_{\rm eISW}$ on the CMB temperature anisotropy power spectrum. Upper panel: CMB temperature anisotropy power spectrum for different values of $A_{\rm eISW}$, specified by the color coding, with the black curve corresponding to the standard case $A_{\rm eISW} = 1$. Notice that, as standard in the field, plotted on the y axis is $T^2_{\rm CMB} D^{TT}_\ell \equiv T^2_{\rm CMB} \ell(\ell+1) C^{TT}_\ell$, with $T_{\rm CMB} \approx 2.725$ K the CMB temperature today. Bottom panel: relative differences between the power spectra shown in the upper panel, relative to the baseline $A_{\rm eISW} = 1$ power spectrum, with the color coding used in the upper panel. It is clear that varying $A_{\rm eISW}$ mostly affects scales around the first acoustic peak, with $A_{\rm eISW} > 0$ ($A_{\rm eISW} < 0$) enhancing (suppressing) power.

can therefore act as a signpost in the large theoretical parameter space of proposed early-time modifications to ΛCDM motivated by the Hubble tension.

III. DATASETS AND METHODOLOGY

In my baseline analysis, I make use of measurements only of CMB temperature anisotropy and polarization power spectra, as well as their cross spectra, from the *Planck* 2018 legacy data release. In particular, I combine the high-ℓ `Plik` likelihood for TT ($30 \leq \ell \lesssim 2500$) as well as TE and EE ($30 \leq \ell \lesssim 2000$), the low-$\ell$ TT-only ($2 \leq \ell < 29$) likelihood based on the COMMANDER component-separation algorithm in pixel space, and the low-ℓ EE-only ($2 \leq \ell < 29$) `SimAll` likelihood [122]. This combination is typically referred to as *Planck* TTTEEE + lowE by the Planck Collaboration, while I will refer to it as *Planck*. Where deemed necessary, I will explicitly remind the reader that it is the high-ℓ `Plik` likelihood which I am making use of, referring to the full CMB dataset as *Planck* (`Plik`).

To assess the robustness of my results, I will also consider combinations of the *Planck* dataset with the following external datasets:

(a) Big bang nucleosynthesis (BBN) prior on $100\omega_b = 2.233 \pm 0.036$, informed by the latest improved measurement of the rate of deuterium burning by LUNA [10]. I refer to this dataset/prior as *BBN*.
(b) Baryon acoustic oscillation measurements from the 6dFGS [95], SDSS-MGS [96], and BOSS DR12 [123] surveys. I refer to this dataset as *BAO*.
(c) Distance moduli measurements in the range $0.01 < z < 2.3$ from the *Pantheon* SNeIa sample [4]. I refer to this dataset as *Pantheon*.

In particular, I will consider the constraints obtained within the *Planck* + *BBN* and *Planck* + *BAO* + *Pantheon* dataset combinations, which I will then compare to the *Planck*-only constraints.

Finally, to further assess the robustness of my results, I replace the `Plik` TTTEEE likelihood with the `CamSpec 12.5HMcl` likelihood, which has access to a larger sky fraction and hence is statistically more powerful (see Ref. [120] for a detailed discussion). When the `CamSpec 12.5HMcl` likelihood is combined with the COMMANDER low-ℓ TT and `SimAll` low-ℓ EE likelihoods, I refer to the resulting combination as *Planck* (`CamSpec`).

In terms of models, I begin by considering a seven-parameter model extending the six-parameter ΛCDM model by allowing the eISW amplitude $A_{\rm eISW}$ to vary. I refer to this model as ΛCDM + $A_{\rm eISW}$. I set a uniform prior in the range $A_{\rm eISW} \in [0;2]$.

To assess the robustness of my results against extensions of this minimal parameter space, I extend the ΛCDM + $A_{\rm eISW}$ model by varying one or two additional parameters which are otherwise fixed to standard values. In particular, the following parameters are varied in addition to the seven standard ones:

(a) The effective number of relativistic degrees of freedom $N_{\rm eff}$, which is otherwise fixed at $N_{\rm eff} = 3.046$.
(b) The primordial helium abundance Y_P, otherwise fixed at the value obtained from standard BBN, given the values of ω_b and $N_{\rm eff}$ (in other words, when varying Y_P, I set `bbn_consistency=F`).
(c) The lensing amplitude $A_{\rm lens}$, which is otherwise fixed at $A_{\rm lens} = 1$.
(d) The running of the scalar spectral index $\alpha_s \equiv dn_s/d\ln k$, which is otherwise fixed at $\alpha_s = 0$.
(e) The running of the scalar spectral index $\beta_s \equiv d\alpha_s/d\ln k = d^2 n_s/d(\ln k)^2$, which is otherwise fixed at $\beta_s = 0$.

Therefore, I consider in total five extended models. Uniform priors are set on $N_{\rm eff} \in [0;10]$, $Y_P \in [0.1;0.5]$, $A_{\rm lens} \in [0;10]$, $\alpha_s \in [-1;1]$, and $\beta_s \in [-1;1]$, as done by the Planck Collaboration. Note that when β_s is varied, I vary α_s as well.

Theoretical predictions for the CMB power spectra and the background expansion are obtained using the Boltzmann solver CAMB [124]. I use Monte Carlo Markov chain (MCMC) methods to sample the posterior distributions for the parameters of the six cosmological models considered (ΛCDM + $A_{\rm eISW}$ as well as the five extensions thereof), using the cosmological sampler `CosmoMC` [125] to generate the MCMC chains. I assess

TABLE I. 68% C.L. constraints on the cosmological parameters of the six-parameter ΛCDM (left column) and seven-parameter $\Lambda\mathrm{CDM} + A_{\mathrm{eISW}}$ (right column) models, obtained from the *Planck* (Plik) dataset alone. The eISW amplitude A_{eISW} is fixed to the standard value $A_{\mathrm{eISW}} = 1$ within the ΛCDM model. The final two rows are separated from the previous rows to highlight the fact that the two associated parameters (H_0 and Ω_m) are derived parameters.

	Planck	
Parameter	ΛCDM	$\Lambda\mathrm{CDM} + A_{\mathrm{eISW}}$
$100\omega_b$	2.235 ± 0.015	2.241 ± 0.020
ω_c	0.1202 ± 0.0013	0.1203 ± 0.0014
θ_s	1.0409 ± 0.0003	1.0409 ± 0.0003
τ	0.0544 ± 0.0078	0.0541 ± 0.0078
$\ln(10^{10}A_s)$	3.045 ± 0.016	3.046 ± 0.016
n_s	0.965 ± 0.004	0.963 ± 0.005
A_{eISW}	1.0	0.988 ± 0.027
$H_0(\mathrm{km/s/Mpc})$	67.26 ± 0.57	67.28 ± 0.62
Ω_m	0.317 ± 0.008	0.317 ± 0.009

the convergence of the MCMC chains by using the Gelman-Rubin parameter $R - 1$ [126] and set the requirement $R - 1 < 0.03$ for the MCMC chains to be considered converged.

IV. RESULTS

I begin by discussing the results obtained within the baseline seven-parameter $\Lambda\mathrm{CDM} + A_{\mathrm{eISW}}$ model from the *Planck* (Plik) dataset alone. In this case, I find $A_{\mathrm{eISW}} = 0.988 \pm 0.027$ at 68% confidence level (C.L.), which is perfectly consistent with the standard ΛCDM expectation of $A_{\mathrm{eISW}} = 1$. The inferred values of the other six parameters are reported in Table I (right column) and compared to their values inferred within the ΛCDM model (where $A_{\mathrm{eISW}} = 1$ is fixed).

From Table I, it is clear that the inferred values of all 6 ΛCDM parameters are extremely stable against the extension where A_{eISW} is allowed to vary, with their uncertainties in most cases barely increasing. This result indicates a simple but very important fact: ΛCDM's prediction for the amplitude of the eISW effect agrees perfectly with the *Planck* data. Conversely, as far as the eISW effect is concerned, there is no obvious sign or need for new physics beyond ΛCDM. As I discussed earlier, and will discuss again later in the context of EDE, this simple observation has important consequences for early-time modifications to ΛCDM, including modifications motivated by attempts to solve the Hubble tension.

The largest parameter shifts are observed for the two parameters most strongly correlated with A_{eISW}, i.e., ω_b and n_s, which, however, shift by no more than 0.3σ when one allows A_{eISW} to vary. In particular, I find A_{eISW} to be negatively correlated with ω_b and positively correlated with n_s. Overall, the most noticeable effect of allowing A_{eISW} to vary is a ≈30% broadening of the uncertainty on ω_b. The reason why A_{eISW} is most strongly correlated with ω_b and n_s can be understood by recalling the effect of these two parameters on the CMB temperature power spectrum (see, e.g., the top right and bottom left panels of Fig. 4.5 of Ref. [127]). Increasing ω_b increases the relative odd/even peak height, with the effect being most noticeable especially for the first peak: the effect is therefore similar to that of increasing A_{eISW}, which explains the negative correlation between these two parameters. Similarly, increasing n_s reduces power on large angular scales (while increasing it on small angular scales), an effect which for scales around the first peak is similar to that of decreasing A_{eISW}, explaining the positive correlation between these two parameters. Moreover, the mild positive correlation existing between ω_b and n_s within ΛCDM is considerably reduced, to the extent of there being almost no correlation, when one varies A_{eISW}.

I now assess the robustness of my results against (i) the inclusion of additional external datasets, or (ii) the use of the CamSpec likelihood in place of Plik in analyzing the high-ℓ *Planck* measurements. The results are summarized in Table II. When one adds the *BBN* prior on ω_b to the baseline *Planck* dataset, the largest improvement is, as expected, for ω_b, whose uncertainty decreases by ≈10%, with the *BBN* prior cutting out part of the parameter space

TABLE II. 68% C.L. constraints on the cosmological parameters of the seven-parameter $\Lambda\mathrm{CDM} + A_{\mathrm{eISW}}$ model obtained from various datasets/dataset combinations, as indicated in the upper section of the Table.

	$\Lambda\mathrm{CDM} + A_{\mathrm{eISW}}$			
Parameter	*Planck* (Plik)	*Planck* (CamSpec)	*Planck* + *BBN*	*Planck* + *BAO* + *Pantheon*
$100\omega_b$	2.241 ± 0.020	2.219 ± 0.020	2.239 ± 0.018	2.251 ± 0.020
ω_c	0.1203 ± 0.0014	0.1197 ± 0.0013	0.1203 ± 0.0013	0.1192 ± 0.0010
θ_s	1.0409 ± 0.0003	1.0411 ± 0.0003	1.0409 ± 0.0003	1.0410 ± 0.0003
τ	0.0541 ± 0.0078	0.0527 ± 0.0083	0.0548 ± 0.0076	0.0557 ± 0.0081
$\ln(10^{10}A_s)$	3.046 ± 0.016	3.038 ± 0.017	3.047 ± 0.016	3.047 ± 0.016
n_s	0.963 ± 0.005	0.969 ± 0.006	0.964 ± 0.005	0.966 ± 0.005
A_{eISW}	0.988 ± 0.027	1.016 ± 0.027	0.993 ± 0.025	0.986 ± 0.027
$H_0(\mathrm{km/s/Mpc})$	67.28 ± 0.62	67.37 ± 0.57	67.26 ± 0.56	67.80 ± 0.47
Ω_m	0.317 ± 0.009	0.314 ± 0.008	0.317 ± 0.008	0.310 ± 0.006

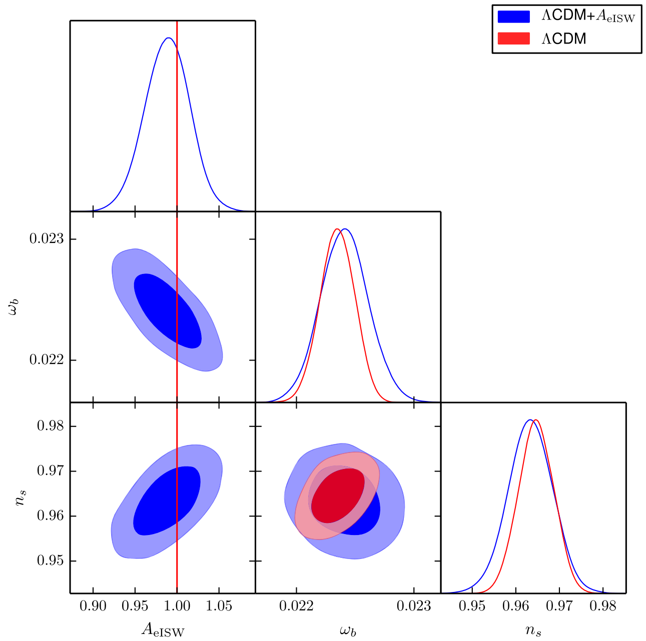

FIG. 2. Triangular plot showing 2D joint and 1D marginalized posterior probability distributions for the eISW amplitude $A_{\rm eISW}$, the physical baryon density ω_b, and the scalar spectral index n_s, obtained from a fit to the *Planck* dataset. The blue contours are obtained within the seven-parameter $\Lambda{\rm CDM} + A_{\rm eISW}$ model, while the red contours are obtained within the six-parameter ΛCDM model, where $A_{\rm eISW}$ is fixed to $A_{\rm eISW} = 1$, as indicated by the vertical red line.

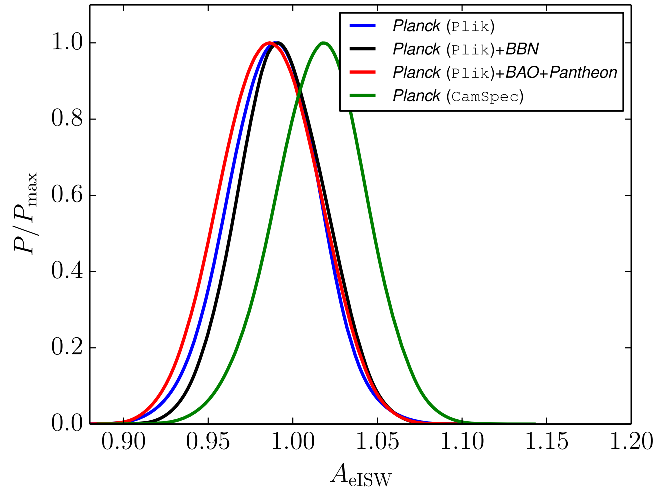

FIG. 3. One-dimensional marginalized normalized posterior distribution for $A_{\rm eISW}$, obtained within the baseline seven-parameter $\Lambda{\rm CDM} + A_{\rm eISW}$ model, from four different datasets/dataset combinations: the baseline *Planck* data using the high-ℓ `Plik` likelihood (blue curve); a combination of *Planck* and a BBN prior on ω_b (black curve); a combination of *Planck* with late-time BAO and *Pantheon* Hubble flow SNeIa measurements (red curve); and the baseline *Planck* data, where the high-ℓ `Plik` likelihood is replaced by the `CamSpec` one (green curve). It is clear that the inferred value of $A_{\rm eISW}$ is very stable overall against these choices of datasets/dataset combinations.

at higher ω_b. Given the direction of the $A_{\rm eISW} - \omega_b$ degeneracy discussed earlier, this results in part of the parameter space at lower $A_{\rm eISW}$ being cut, as well as the corresponding parameter uncertainty slightly decreasing. From the *Planck+BBN* dataset combination, I infer $A_{\rm eISW} = 0.993 \pm 0.025$, which further improves the consistency with the standard value $A_{\rm eISW} = 1$.

Qualitatively similar results are obtained when one considers the *Planck+BAO+Pantheon* dataset combination. While larger parameter shifts are observed than in the previous case, these remain small overall, and still well below the 1σ level. In particular, I infer $A_{\rm eISW} = 0.986 \pm 0.027$, which is still perfectly consistent with the standard value $A_{\rm eISW} = 1$.

Finally, I again consider the *Planck* data alone, but this time adopt the `CamSpec` likelihood in place of the `Plik` high-ℓ (*TTTEEE*) one. In this case, I find larger parameter shifts, although again these all remain relatively small, always below the 1σ level. The magnitudes of these shifts are consistent with those reported by the Planck Collaboration [5] and investigated in Ref. [120]. The largest observed shift is a $\approx 0.8\sigma$ shift toward lower values of ω_b. Again, given the previously discussed mutual degeneracies between ω_b, n_s, and $A_{\rm eISW}$, this shift in ω_b is unsurprisingly accompanied by correlated shifts in n_s and $A_{\rm eISW}$ toward larger values. Overall, the inferred value of $A_{\rm eISW} = 1.016 \pm 0.027$ remains in excellent agreement with the standard value $A_{\rm eISW} = 1$.

The main message is therefore that the *Planck*-only result, which sees remarkable consistency between the inferred value of $A_{\rm eISW} = 0.988 \pm 0.027$ and the standard value of $A_{\rm eISW} = 1$, is very stable against (i) the addition of external datasets (*BBN* and *BAO+Pantheon*), and (ii) the choice of high-ℓ *Planck* likelihood (`Plik` or `CamSpec`). A visual representation of these results is given in Fig. 3, where I plot the 1D marginalized $A_{\rm eISW}$ posterior distributions within the $\Lambda{\rm CDM} + A_{\rm eISW}$ model given all the dataset combinations/choices discussed.

I now assess the robustness of the previous results against extended parameter spaces, considering the one- and two-parameter extensions discussed in Sec. III. The results are reported in Table III, which focuses only on ω_b, n_s, $A_{\rm eISW}$, and, of course, the additional parameters themselves. I have chosen to vary $N_{\rm eff}$, Y_P, $A_{\rm lens}$, α_s, and β_s, as these are the parameters I expect to be the most strongly correlated with $A_{\rm eISW}$ (for reasons similar to those previously discussed for ω_b and n_s).

Overall, I find that the inferred value of $A_{\rm eISW}$ is very stable against these extensions. The largest shifts are observed when one allows $A_{\rm lens}$ to vary. This is hardly surprising given that the *Planck* data appear to show a moderate preference for $A_{\rm lens} > 1$: this lensing anomaly (and the closely related apparent preference for a spatially closed Universe from *Planck* primary CMB data) is an

TABLE III. As in Table II, but focused on one- and two-parameter extensions of the baseline seven-parameter $\Lambda\mathrm{CDM} + A_{\mathrm{eISW}}$ model, with the extra parameters being the effective number of relativistic species N_{eff}, the primordial helium fraction Y_P, the lensing amplitude A_{lens}, the running of the scalar spectral index α_s, and the running of the running of the scalar spectral index β_s. Note that whenever β_s is varied, α_s is varied as well. These extra parameters are indicated by X in the parameters column. The row labeled "X ($A_{\mathrm{eISW}} = 1$)" reports constraints on the extra parameter(s) X within the seven- or eight-parameter $\Lambda\mathrm{CDM} + X$ model, where A_{eISW} is fixed to the standard value $A_{\mathrm{eISW}} = 1$.

	Planck					
Parameter	$\Lambda\mathrm{CDM} + A_{\mathrm{eISW}}$	$+N_{\mathrm{eff}}$	$+Y_P$	$+A_{\mathrm{lens}}$	$+\alpha_s$	$+\alpha_s + \beta_s$
$100\omega_b$	2.241 ± 0.020	2.225 ± 0.028	2.234 ± 0.025	2.275 ± 0.024	2.243 ± 0.020	2.243 ± 0.021
n_s	0.963 ± 0.005	0.958 ± 0.009	0.961 ± 0.008	0.969 ± 0.005	0.963 ± 0.006	0.958 ± 0.007
A_{eISW}	0.988 ± 0.027	0.994 ± 0.029	0.991 ± 0.029	0.975 ± 0.027	0.992 ± 0.027	0.978 ± 0.030
X	$\cdots$	2.89 ± 0.19	0.239 ± 0.013	1.192 ± 0.065	-0.006 ± 0.007	$0.005 \pm 0.011, 0.017 \pm 0.014$
X ($A_{\mathrm{eISW}} = 1$)	$\cdots$	2.92 ± 0.19	0.240 ± 0.013	1.180 ± 0.065	-0.006 ± 0.007	$0.001 \pm 0.010, 0.012 \pm 0.013$

issue which is well known and well documented in the literature (see, e.g., Refs. [120,122,128–140]). However, even within the $\Lambda\mathrm{CDM} + A_{\mathrm{eISW}} + A_{\mathrm{lens}}$ model, the associated parameter shifts relative to the $\Lambda\mathrm{CDM} + A_{\mathrm{eISW}}$ model (with $A_{\mathrm{lens}} = 1$ fixed) remain small. The largest observed shift is for ω_b, which increases by $\approx 1\sigma$. On the other hand, A_{eISW} decreases by $\approx 0.3\sigma$ to $A_{\mathrm{eISW}} = 0.975 \pm 0.027$ but still remains perfectly consistent with the standard value $A_{\mathrm{eISW}} = 1$ within better than 1σ.

Shifts of comparable magnitude are observed in n_s and A_{eISW} when one allows α_s and β_s to vary. In particular, within the $\Lambda\mathrm{CDM} + A_{\mathrm{eISW}} + \alpha + \beta_s$ model, I infer $A_{\mathrm{eISW}} = 0.978 \pm 0.030$, which also remains perfectly consistent with the standard value $A_{\mathrm{eISW}} = 1$ within better than 1σ, accompanied by $\approx 1\sigma$ hints for nonzero β_s. As discussed in Ref. [141], the 1σ hint for nonzero β_s, already reported by the Planck Collaboration [5], is due to the fact that a positive β_s provides a slightly better fit to the low-ℓ part of the CMB power spectrum. While it remains consistent with $\alpha_s = 0$ within 1σ, the slight preference for negative α_s when this parameter is varied and β_s is fixed is instead related to the mild tensions between high-ℓ and low-ℓ multipoles in the CMB temperature power spectrum, as discussed in Refs. [5,142].

Overall, the main message here is that the inferred value of A_{eISW}, being highly consistent with the standard value $A_{\mathrm{eISW}} = 1$ obtained within the baseline $\Lambda\mathrm{CDM} + A_{\mathrm{eISW}}$ model, is very stable against the minimal one- and two-parameter extensions I have studied. A visual representation of these results is given in Fig. 4, where I plot the 1D marginalized A_{eISW} posterior distributions obtained from the *Planck* dataset given the baseline and extended models considered.

These results place important restrictions on early-time new physics models, for instance, those invoked to address the Hubble tension. Clearly, in order to fit the CMB data well, these models will need to make a prediction for the eISW effect which is similar to, or at least not too distant from, that of ΛCDM. Since a non-negligible amount of early-time new physics is required to significantly alleviate the Hubble tension, the resulting impact on the eISW effect is expected to be equally non-negligible, thereby posing a significant challenge to these models. One possible solution is that of shifting the values of some of the standard ΛCDM parameters (such as ω_c) in order to readjust the eISW amplitude, a shift which, however, may come at the price of degrading the fit to other datasets. In the following section, I will provide a case study of early dark energy, with the goal of illustrating the challenges that it faces in relation to the eISW effect, as anticipated in Sec. I.

Note that at least three earlier works previously introduced A_{eISW}, constrained to $A_{\mathrm{eISW}} = 0.979 \pm 0.055$ from

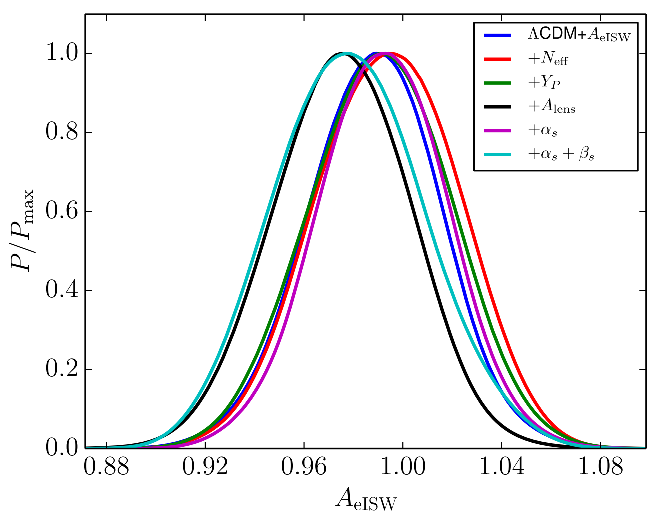

FIG. 4. One-dimensional marginalized normalized posterior distribution for A_{eISW}, obtained from the *Planck* data, within the baseline seven-parameter $\Lambda\mathrm{CDM} + A_{\mathrm{eISW}}$ model (blue curve), as well as extensions where the following parameters are allowed to vary as well: the effective number of relativistic species N_{eff} (red curve), the helium fraction Y_P (green curve), the lensing amplitude A_{lens} (black curve), the running of the scalar spectral index α_s (magenta curve), and both the running α_s and the running of the scalar spectral index β_s (cyan curve). It is clear that the inferred value of A_{eISW} is very stable overall against these parameter space extensions.

WMAP7 + SPT [117], to $A_{\mathrm{eISW}} = 1.06 \pm 0.04$ from the *Planck* 2015 temperature and large-scale polarization data [118], and to $A_{\mathrm{eISW}} = 1.064 \pm 0.042$ from the *Planck* 2018 temperature data alone [119]. It is, of course, worth revisiting these constraints (i) in light of the full *Planck* 2018 legacy release data (including polarization data and assessing the stability of the results against a different choice of high-ℓ *Planck* likelihood [120]), and (ii) in view of the Hubble tension and the possible implications of the results for early-time new physics. Concerning (i), particularly crucial are the inclusion of small-scale *TTTEEE* polarization data, and the significant improvements which led to the `SimAll` large-scale *EE* likelihood. As discussed in detail in Ref. [143], the TE cross spectrum is remarkably good at constraining ω_b, while the EE power spectrum is extremely good at constraining ω_b, ω_c, and n_s, and, in particular, at breaking the $\omega_b - n_s$ degeneracy (due to the fact that the amplitude of the EE power spectrum is sensitive to c_s^2, the square of the photon-baryon sound speed). This is particularly true when the TE and EE spectra are combined with measurements of the TT power spectrum, as this combination is very efficient at breaking degeneracies between the main cosmological parameters. However, EE alone is already able to constrain ω_b, ω_c, and n_s as well as or better than TT, even at a lower signal-to-noise level [143].

For the reasons discussed above, the use of the latest large- and small-scale polarization data included in this analysis is crucial to further improving the constraints on A_{eISW}. This results in an uncertainty which is reduced by up to a factor of 2 compared to the results of the previously published Refs. [117–119], while the central value of A_{eISW} is also in better agreement with the standard value $A_{\mathrm{eISW}} = 1$.

Future Stage III and Stage IV CMB experiments (mostly ground based) will significantly improve CMB power spectrum measurements compared to *Planck*, especially insofar as the E-mode power spectrum is concerned, significantly improving constraints on the base ΛCDM parameters. As far as ω_b and n_s are concerned, their determinations will improve by up to a factor of 2 for stage III experiments such as Simons Observatory (see Table 3 of Ref. [144]) and by up to a factor of 3 or more for planned stage IV experiments such as CMB-S4 (see Table 8-1 of Ref. [145]). While a fully fledged forecast is beyond the scope of this paper, I expect comparable improvements in the achievable A_{eISW} sensitivity. This means that A_{eISW} might potentially be inferred to $\lesssim 1\%$ precision from stage IV experiments: this would set even more important limits on the extent to which early-time new physics can operate.

V. EARLY ISW EFFECT AND NEW PHYSICS: CASE STUDY WITH EARLY DARK ENERGY

In this section, I will discuss how the previous results affect early-time new physics in practice. For convenience, I will present a case study focused on the eISW effect in EDE models (see, e.g., Refs. [17–42] for examples of EDE models). The arguments I will present in this section, however, are likely to apply more broadly than just to EDE, but more generally to most models whose effect is to enhance the expansion rate around recombination.

Early dark energy is among the most promising (or "least unlikely" in the words of Ref. [101]) proposed solutions to the Hubble tension. EDE falls within a class of models which increase the expansion rate just prior to recombination. This reduces the sound horizon at last scattering, allowing for a higher H_0 from CMB data without running afoul of late-time constraints from BAO and Hubble flow SNeIa. In the implementation I will consider here, the role of EDE is played by an ultralight scalar field with mass of order $\mathcal{O}(10^{-27})$ eV. At early times, the field is displaced from the minimum of its potential while being held in place by Hubble friction, therefore behaving as an effective dark energy component. Once the expansion rate drops below the mass of the field, Hubble friction is no longer important and the field is free to roll down the potential and oscillate around the minimum. If the potential around the minimum is sufficiently steep (in particular, steeper than quartic), EDE then redshifts faster than radiation and rapidly becomes a subdominant component of the Universe's energy budget.

Consider an EDE axion-like field ϕ, i.e., a pseudoscalar enjoying a global $U(1)$ shift symmetry, broken by nonperturbative effects generating a potential $V(\phi)$, which in turn dictates the dynamics of the EDE field.[2] Here I will consider a potential of the form

$$V(\phi) = m^2 f^2 \left(1 - \cos\left(\frac{\phi}{f}\right)\right)^n, \tag{3}$$

where m is a mass scale and f is the EDE decay constant, at which the global $U(1)$ symmetry is broken. A potential of this form requires a careful fine-tuning of the hierarchy of instanton actions [151,152], but for integer values of n the fine-tuning is restricted to the first n terms. I will fix $n = 3$, as this is the minimum integer value which allows EDE to redshift faster than radiation once the field reaches the minimum of the potential. At its minimum, the potential is locally $V \propto \phi^6$, so the subsequent effective equation of state of EDE is $w_{\mathrm{EDE}} = 1/2$. The dynamics of the EDE field in an expanding Universe is governed by the Klein-Gordon equation as follows:

[2]This type of EDE field could arise from the so-called string axiverse [146–150], featuring multiple axionlike particles spanning various decades in mass.

$$\ddot{\phi} + 3H\dot{\phi} + \frac{dV(\phi)}{d\phi} = 0, \tag{4}$$

with the dot denoting a derivative with respect to time.

The cosmological dynamics of this EDE model are more simply described in terms of three parameters: the initial field displacement (or misalignment angle) $\theta_i = \phi_i/f$, with ϕ_i being the initial value at which ϕ is held by Hubble friction, as well as the "critical redshift" z_c and the "EDE fraction" $f_{\rm EDE}$. More specifically, at the critical redshift z_c, which approximately corresponds to the moment just before the field starts to oscillate around its minimum, EDE provides its maximum fractional contribution to the energy budget of the Universe $f_{\rm EDE} \equiv \rho_{\rm EDE}(z)/(3M_{\rm Pl}^2 H^2(z))|_{z=z_c}$, with $\rho_{\rm EDE}(z)$ and $M_{\rm Pl}$ being the EDE energy density and reduced Planck mass, respectively. Alleviating the Hubble tension requires an EDE fraction of order $f_{\rm EDE} \simeq 10\%$.

To illustrate the issues EDE faces in relation to the eISW effect, I will consider a numerical example closely following that of Ref. [25] which focuses on $n = 3$ EDE. I will compare EDE to ΛCDM, with the parameters of both models in this numerical example being summarized in Table IV. The EDE parameters (right column) are set to their best-fit values as determined from a fit to *Planck*, BAO, *Pantheon*, and redshift-space distortions measurements, alongside a SH0ES prior on H_0, as reported in Ref. [18]. The key to the success of the EDE proposal is its ability to accommodate a higher value of H_0 while fitting the CMB power spectra as well as ΛCDM (with a lower H_0). In the context of this numerical example, the ΛCDM parameters (left column) are chosen so that the resulting CMB power spectra are essentially indistinguishable from those within the EDE model.

As can clearly be seen from Table IV, and as already noted elsewhere (see, e.g., Refs. [18,25]), the fact that EDE can accommodate a higher H_0 while preserving the fit to CMB data comes at the cost of important shifts in some of the standard ΛCDM parameters. In particular, both ω_c and n_s need to increase, rather substantially in the case of ω_c. To show the importance of the increase in ω_c, in Fig. 5 I show the resulting ΛCDM and EDE temperature power spectra, with parameters as given in Table IV, with the EDE model with low (high) ω_c given in the left (right) panel. The corresponding bottom panels show the relative differences in the EDE power spectrum relative to ΛCDM. Figure 5 has been produced using `CLASS_EDE` [25],[3] a modified version of the Boltzmann solver CLASS [153].

In Fig. 5 we see that an EDE model with low ω_c predicts excess power, particularly around the first acoustic peak, and more generally for all multipoles $\ell \gtrsim 100$. The power spectrum of the EDE model with high ω_c, however, is essentially indistinguishable from the ΛCDM one. In both models, the slight decrease of power at large scales ($\ell \lesssim 30$) is swamped by cosmic variance and hence virtually impossible to observe. Analogous effects are observed in the CMB polarization power spectra and temperature-polarization cross spectra, which for conciseness I do not show here.

[3]Available at github.com/mwt5345/class_ede.

TABLE IV. Values of the cosmological parameters used in the numerical example comparing ΛCDM against two EDE models in Sec. V (see Figs. 5 and 6). The difference between the two EDE models is in the value of the physical cold DM density ω_c, which is fixed to $\omega_c = 0.1320$ in the "high" case (middle column), and to $\omega_c = 0.1177$ (as in the ΛCDM model it is being compared against) in the "low" case (right column).

Parameter	ΛCDM	EDE (high ω_c)	EDE (low ω_c)
$100\omega_b$	2.253	2.253	2.253
ω_c	0.1177	0.1322	0.1177
H_0(km/s/Mpc)	68.21	72.19	72.19
τ	0.085	0.072	0.072
$\ln(10^{10}A_s)$	3.0983	3.0978	3.0978
n_s	0.9686	0.9889	0.9889
$f_{\rm EDE}$	...	0.122	0.122
$\log_{10} z_c$	...	3.562	3.562
θ_i	...	2.83	2.83
n	...	3	3

The physical origin of the shift in ω_c can be traced back to the effect of EDE during the time when its contribution to the Universe's energy budget is non-negligible. During this time, the increase in the expansion rate brought upon by EDE suppresses the growth of perturbations: this is analogous to how cosmic acceleration at late times also suppresses the growth of structure. To preserve the fit to the CMB power spectra, this needs to be accompanied by an increase in ω_c which compensates for the decreased efficiency in the growth of the structure.[4] The increase in ω_c, however, directly increases the late-time amplitude of the matter fluctuations σ_8, exacerbating the discrepancy between CMB and WL probes, and degrading the fit to LSS clustering data. This degraded fit to WL and LSS data ultimately limits the success of the EDE proposal in solving the Hubble tension [25,30,31] (see, however, a partial rebuttal of these results in Refs. [34,35]).

Here, I will show that these shifts in ω_c are essentially required to preserve the amplitude of the eISW effect predicted by ΛCDM, which perfectly fits the *Planck* data, as per my earlier results discussed in Sec. IV, inferring that $A_{\rm eISW}$ is remarkably consistent with the standard value $A_{\rm eISW} = 1$. Let us focus on the EDE model with low ω_c, which I argue increases the amplitude of the eISW effect

[4]A smaller increase in n_s is instead also needed to compensate for the scale-dependent suppression of growth due to the fact that EDE is dynamically relevant for only a short amount of time.

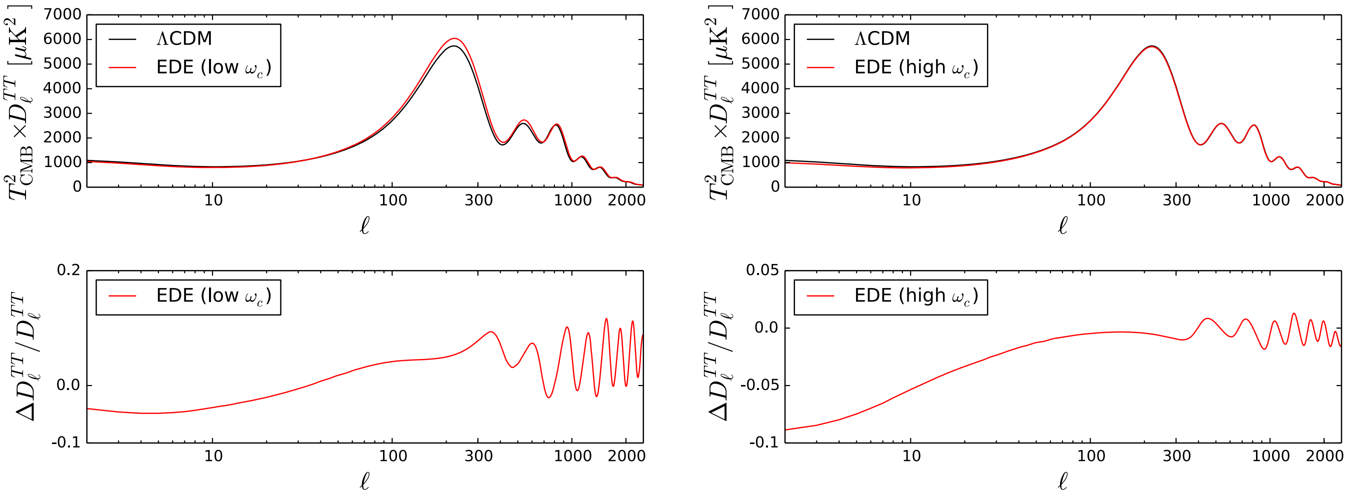

FIG. 5. CMB temperature anisotropy power spectra for ΛCDM and early dark energy (EDE). Top left panel: CMB temperature anisotropy power spectrum for a ΛCDM model (black curve) with parameters given by the left column of Table IV, and for an EDE model (red curve) with parameters given by the middle column of Table IV, where, in particular, the physical cold DM density is fixed to the low value $\omega_c = 0.1177$. Bottom left panel: relative differences between the EDE and ΛCDM power spectra shown in the upper panel, with the former clearly predicting an excess of power compared to the latter, particularly around the scale of the first peak. Right panel: as in the left panel, but with the EDE parameters given by the right column of Table IV, where, in particular, the physical cold DM density is fixed to the high value $\omega_c = 0.1320$. As the lower panel shows, this increase in ω_c makes the two power spectra nearly indistinguishable.

compared to ΛCDM (with the same value of ω_c). This comes about for two reasons, working at the perturbation and background levels, respectively:

(a) At the perturbation level, the EDE-induced suppression of the growth of perturbations is accompanied by a related enhanced decay of the gravitational potentials Φ and Ψ, which decay more quickly than they would if the Universe were filled with radiation alone. This leads to a scale-dependent enhancement of the eISW effect. The increase in ω_c helps counteract this enhanced decay of the gravitational potentials.

(b) At the background level, the presence of an extra component delays the onset of matter domination. This increases the time over which gravitational potentials vary with time, leading to a global enhancement of the eISW effect. The increase in ω_c helps counteract this effect by anticipating the onset of matter domination.

Note that the two effects are similar in that increasing the energy density of dark energy at late times enhances the decay of gravitational potentials and anticipates the onset of dark energy domination, leading to an enhanced late ISW effect, visible in the low-ℓ part of CMB temperature power spectrum or, more clearly, in cross-correlations between CMB and LSS probes [154–158]. The first of the two points above, i.e., the excess decay of the Weyl potential $\Phi - \Psi$, was first pointed out in the context of an EDE-type model in Ref. [54]; see also Sec. III. E and Fig. 8 of Ref. [29] in the context of the related new EDE (NEDE) model (the different sign convention in the perturbed line element means that the Weyl potential in Ref. [29] is given by $\Phi + \Psi$ rather than $\Phi - \Psi$).

Besides these two physical effects enhancing the eISW amplitude, there is potentially a third effect which comes into play purely at the perturbation level. As first pointed out in Refs. [29,54], once EDE starts decaying, the decaying fluid supports its own acoustic oscillations, which in turn source the gravitational potential. The subsequent Jeans stabilization of these acoustic oscillations then leads to an enhanced decay of the Weyl potential, which in turn enhances the eISW effect. This effect can be clearly seen in Fig. 8 of Ref. [29] to the right of the vertical dotted line (whereas the previous two effects show up to the left thereof). It is worth noting that, while the previous two physical effects apply to generic EDE implementations, this third effect is significantly more model dependent and depends on specific details of the EDE model, such as sound speed, perturbation mode, trigger dynamics, and viscosity parameter.

To confirm that the observed shifts in ω_c are indeed required to reduce the amplitude of the eISW effect, I produce plots comparing ΛCDM and EDE that are analogous to those in Fig. 5, this time isolating the eISW contribution to the CMB temperature power spectrum, $C_\ell^{TT,\rm eISW}$. The result is shown in Fig. 6, from which one clearly sees that an EDE model with low ω_c (left panel) predicts an enhanced eISW effect on all scales. In particular, I find a nearly 20% excess in the eISW power on multipoles $\ell \lesssim 500$ that is particularly evident around the scale of the first peak (see the left panel of Fig. 5). Raising ω_c (right panel) considerably suppresses this effect, leading to an excess in eISW power at the $\mathcal{O}(3\%)$ level, which in turn significantly improves the fit to the CMB temperature

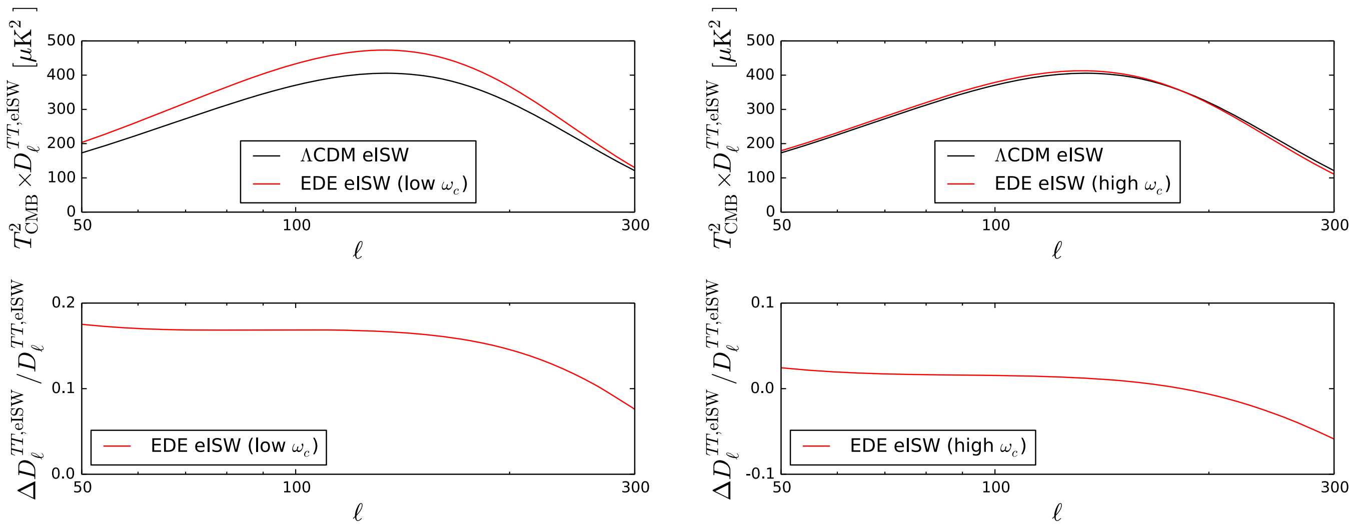

FIG. 6. Like Fig. 5 but focusing on the early ISW (eISW) contribution to the CMB temperature anisotropy power spectrum. It is clear that the increase in ω_c significantly decreases the excess eISW contribution on most scales of interest. Note that the x axis covers multipoles only in the range $50 < \ell < 300$, where the eISW effect is most prominent, as shown in Fig. 1.

power spectrum, leading to predictions which are essentially indistinguishable from those of ΛCDM (see the right panel of Fig. 5).

As my earlier results in Sec. IV have shown, a $\mathcal{O}(20\%)$ increase in the eISW effect is excluded at $>5\sigma$ by the *Planck* measurements, and therefore needs to be counteracted by means of shifts in some of the standard ΛCDM parameters, in this case ω_c. My results in this section, particularly Fig. 6, therefore show that, if the increase in ω_c (and the corresponding worsened fit to WL and LSS data) leads to the demise of the EDE scenario in terms of solving the Hubble tension (modulo the rebuttal arguments discussed in Refs. [34,35]), it is really the eISW effect which ultimately is to blame. More precisely, what is to "blame" is the fact that ΛCDM's prediction for the eISW effect is in excellent agreement with the *Planck* measurements, which show no obvious evidence for new physics at early times.

Are the EDE-specific arguments presented here more general, i.e., do they apply more generally to other early-time new physics scenarios? I believe that the answer is yes, at least insofar as this early-time new physics increases the expansion rate around recombination. In fact, from very general considerations one can expect that this type of early-time new physics will (i) lead to a decay of the gravitational potentials (much like dark energy at late times), and (ii) slow down the growth of perturbations. To confirm this, one should solve the equation governing the time evolution of gravitational potentials, which is generically given by (see, e.g., Ref. [159])

$$k^2\Phi + 3\mathcal{H}(\dot{\phi} - 3\mathcal{H}\Psi) = 4\pi G a^2 \sum_i \rho_i \delta_i, \qquad (5)$$

with $\mathcal{H}$ being the conformal Hubble rate, G being Newton's constant, a being the scale factor, the dot denoting a derivative with respect to conformal time η, and the sum on the right-hand side running over all components contributing to the Universe's energy budget, with energy densities and density contrasts given by ρ_i and δ_i, respectively. Approximate solutions to Eq. (5) are known only for idealistic situations where the Universe is dominated by a single component, e.g., deep in the matter era $[\Phi(\eta) = \text{const}]$ or deep in the radiation era $(\Phi(\eta) \propto [\sin(\eta) - \eta\cos(\eta)]/\eta^3)$. In all other situations, including the simultaneous presence of radiation, matter, and a new component at early times (such as EDE), Eq. (5) needs to be solved numerically. However, given the form of Eq. (5), it is reasonable to expect that any component whose effect is to speed up (even if only slightly) the expansion of the Universe, and hence raise $\mathcal{H}$, will contribute to the decay of Φ, which in itself is already decaying during the radiation-dominated era, thus enhancing the eISW effect.

Similarly, the equation for the growth of matter perturbations δ does not take a simple closed form in a generic Universe where radiation, matter, and a new component at early times are simultaneously present. However, if the new component is subdominant, the equation governing δ should approximately reduce to the form

$$\ddot{\delta} + \frac{\dot{\delta}}{\eta} = \mathcal{S}(k,\eta), \qquad (6)$$

with the source term $\mathcal{S}(k,\eta)$ given by

$$\mathcal{S}(k,\eta) = -3\ddot{\Phi} + k^2\Phi - \frac{3\dot{\Phi}}{\eta}. \qquad (7)$$

Given the previous considerations on the behavior of Φ in the presence of a new component speeding up the expansion of the Universe, and the form of Eqs. (6) and (7), one can generically expect δ to grow more slowly in the presence of such a component.

I wish to clarify that the arguments presented above concerning the enhanced decay of potentials and reduced growth of perturbations are not a rigorous no-go theorem, nor is it my intention to elevate them to such a degree. While I expect these arguments to hold generically for models which decrease the sound horizon by introducing a new dark energy–like component, or in any case through a speedup of the expansion of the Universe around recombination, I stress that the validity of these conclusions should be checked on a case-by-case basis for each given model. Note that a similar argument (at a similar level of rigor) was also presented in Ref. [25]. In any case if, as I expect, these arguments apply more generically to models beyond EDE, I would also expect these models to have to compensate for the enhanced eISW effect. The most direct, but by no means only, way of doing so would be to raise ω_c, which, however, would exacerbate the S_8 discrepancy,[5] worsening the fit to WL and LSS clustering measurements and possibly leading to the demise of these models.

However, model-dependent aspects make it important to assess the details of early-type models on a case-by-case basis to judge their prospects. Specific early-type models may be able to introduce ingredients which can at least partially counteract the enhanced eISW effect. The NEDE model is an example in this sense (see the discussion in Ref. [33]), as it does not significantly worsen the S_8 discrepancy already present within ΛCDM. Another example is that of the Majoron model, which can damp neutrino free streaming and inject additional energy density into the neutrino sector prior to recombination, thereby enhancing the pre-recombination expansion rate [161] and requiring an increase in ω_c. However, these neutrino-Majoron interactions leave peculiar imprints in the low-ℓ part of the CMB power spectrum, where the eISW effect is relevant (see Fig. 5 of Ref. [161]): these imprints might be partially responsible for the model's good performance in solving the Hubble tension when confronted against CMB and LSS data, despite the increase in ω_c. The NEDE and Majoron cases are just two examples of models introducing specific model-dependent ingredients which can partially counteract the two effects I previously identified as being responsible for the enhanced eISW effect: other ingredients which also do so are, of course, possible. However, it is likely that these ingredients will not be able to fully resolve the discrepancies between CMB and LSS/WL data already present within ΛCDM, and that further extensions will be required to do so.[6]

Other types of early-time new physics which accommodate a higher H_0 without speeding up the expansion of the Universe around recombination should be immune to these conclusions, although they are, of course, subject to stringent constraints from the full CMB power spectra. One example is the strongly interacting neutrino model [50], whose worsened fit to CMB polarization measurements limits its success in solving the Hubble tension [89,91,92], although it is worth noting that the preference for a higher value of $N_{\rm eff}$ within this model indirectly leads to an enhancement of the pre-recombination expansion rate.

My overall findings are similar in spirit to those of recent works along a related line, which question the ability of early-time new physics, or, more precisely, early-time new physics lowering the sound horizon alone, to fully resolve the Hubble tension [109–115]. There is, of course, no question about the fact that late-time new physics *alone* falls short of fully solving the Hubble tension due to constraints imposed by BAO and SNeIa measurements [97–103] (with the possible exception of models invoking local effects such as those considered in Refs. [162–168]). My results, alongside those of Refs. [109–115] (though perhaps less model independent than the latter), show that early-time new physics models face equally severe (if not more severe) stumbling blocks as late-time new physics ones.

VI. CONCLUSIONS

Why does ΛCDM fit CMB measurements so well? Why is there no evidence for new physics from CMB data alone? The answers to these questions, and to other general model-agnostic questions testing the consistency of ΛCDM, can provide a compass for navigating the *mare magnum* which is the theory space of proposed solutions to the Hubble tension. Early-time new physics, particularly models which raise the expansion rate around recombination to lower the sound horizon, should leave an important imprint on the eISW effect, which should typically be enhanced. Motivated by this, I have performed an eISW-based consistency test of ΛCDM by introducing the phenomenological scaling parameter $A_{\rm eISW}$, artificially rescaling the amplitude of the eISW contribution to the CMB power spectra.

[5]See, however, Ref. [160] for a recent work arguing that the S_8 discrepancy may be compatible with a statistical fluctuation.

[6]In the context of NEDE, these ingredients could include interactions between the scalar field and the visible sector and/or a significant amount of oscillations around the new vacuum after the phase transition, all of which affect the way the Weyl potential decays, and therefore the way in which the eISW effect is enhanced (see, e.g., the discussion toward the end of Ref. [33]).

From a fit to the *Planck* 2018 legacy data release temperature and polarization data within a seven-parameter $\Lambda\mathrm{CDM} + A_{\mathrm{eISW}}$ model, I infer $A_{\mathrm{eISW}} = 0.988 \pm 0.027$, which is in perfect agreement with the standard value $A_{\mathrm{eISW}} = 1$. This result shows that ΛCDM's prediction for the eISW effect is in perfect agreement with data, and there is room for no more than an $\approx 3\%$ enhancement/suppression of the eISW effect relative to this prediction. More crucially, this result poses important restrictions on early-time new physics models, which will need to (approximately) match this prediction.

I have illustrated the implications of these results for new physics focusing on the well-known EDE model. For EDE to fit CMB data as well as ΛCDM while accommodating a higher H_0, an increase in ω_c is required—this has been argued to worsen the fit to WL and galaxy clustering measurements, leading to the conclusion that EDE fails to restore cosmic concordance. I have explicitly shown that the increase in ω_c is required to bring the amplitude of the eISW effect (which would otherwise be overpredicted by $\approx 20\%$) into better agreement with ΛCDM's prediction. I have argued that this problem should go beyond EDE and be a general feature of early-time new physics, at least for models which raise the expansion rate around recombination.

My findings join further existing restrictions concerning the ability of early-time new physics lowering the sound horizon alone to fully resolve the Hubble tension [109–115]. On the other hand, the late-time expansion history is too well constrained by BAO and uncalibrated SNeIa measurements for late-time new physics to be able to fully resolve the Hubble tension on their own [97–103]. Overall, this suggests that a definitive resolution of the Hubble tension might require one or more of the following: (i) a combination of modifications to ΛCDM, at both early and late times, (ii) highly nontrivial early-time modifications to ΛCDM which are able to match ΛCDM's prediction for the eISW effect while not degrading the fit to other datasets, (iii) local new physics (in agreement with the findings of Ref. [111] and including models of the types proposed in Refs. [163,165–168]), or (iv) convincingly identifying systematic errors in one or more of the involved datasets (see, e.g., Refs. [169–171]).

It is, of course, entirely possible that clear signs of new physics will appear in future CMB data [144,145,172]. In that case, whatever emerges will undoubtedly teach us something fundamental about nature. Until then, however, general consistency tests of ΛCDM will keep providing important taffrails while steering through the vast sea that is the theory space of new physics.

ACKNOWLEDGMENTS

I am grateful to George Efstathiou for many useful discussions which led to the development of this work, and for encouraging me to think about general consistency tests of ΛCDM. I thank Alex Reeves, Janina Renk, and Blake Sherwin for very useful discussions around the subject of this work and for help with the codes, Josh Kable for bringing a very relevant work to my attention, and Florian Niedermann and Martin Sloth for valuable comments on a previous draft. I am supported by the Isaac Newton Trust and the Kavli Foundation through a Newton-Kavli Fellowship, and by a grant from the Foundation Blanceflor Boncompagni Ludovisi, née Bildt. I acknowledge a College Research Associateship at Homerton College, University of Cambridge. This work was performed using resources provided by the Cambridge Service for Data Driven Discovery (CSD3), operated by the University of Cambridge Research Computing Service [173], provided by Dell EMC and Intel using Tier 2 funding from the Engineering and Physical Sciences Research Council (Capital Grant No. EP/P020259/1), and DiRAC funding from the Science and Technology Facilities Council [174].

[1] A. G. Riess *et al.* (Supernova Search Team), Astron. J. **116**, 1009 (1998).
[2] S. Perlmutter *et al.* (Supernova Cosmology Project), Astrophys. J. **517**, 565 (1999).
[3] M. A. Troxel *et al.* (DES Collaboration), Phys. Rev. D **98**, 043528 (2018).
[4] D. M. Scolnic *et al.*, Astrophys. J. **859**, 101 (2018).
[5] N. Aghanim *et al.* (Planck Collaboration), Astron. Astrophys. **641**, A6 (2020).
[6] F. Bianchini *et al.* (SPT Collaboration), Astrophys. J. **888**, 119 (2020).
[7] S. Aiola *et al.* (ACT Collaboration), J. Cosmol. Astropart. Phys. 12 (2020) 047.
[8] S. Alam *et al.* (eBOSS Collaboration), Phys. Rev. D **103**, 083533 (2021).
[9] M. Asgari *et al.* (KiDS Collaboration), Astron. Astrophys. **645**, A104 (2021).
[10] V. Mossa *et al.*, Nature (London) **587**, 210 (2020).
[11] V. Sahni, Lect. Notes Phys. **653**, 141 (2004).
[12] G. Bertone, D. Hooper, and J. Silk, Phys. Rep. **405**, 279 (2005).
[13] D. Huterer and D. L. Shafer, Rep. Prog. Phys. **81**, 016901 (2018).

[14] L. Verde, T. Treu, and A. G. Riess, Nat. Astron. 3, 891 (2019).
[15] E. Di Valentino, O. Mena, S. Pan, L. Visinelli, W. Yang, A. Melchiorri, D. F. Mota, A. G. Riess, and J. Silk, Classical Quantum Gravity 38, 153001 (2021).
[16] L. Perivolaropoulos and F. Skara, arXiv:2105.05208.
[17] E. Mörtsell and S. Dhawan, J. Cosmol. Astropart. Phys. 09 (2018) 025.
[18] V. Poulin, T. L. Smith, T. Karwal, and M. Kamionkowski, Phys. Rev. Lett. 122, 221301 (2019).
[19] P. Agrawal, F.-Y. Cyr-Racine, D. Pinner, and L. Randall, arXiv:1904.01016.
[20] S. Alexander and E. McDonough, Phys. Lett. B 797, 134830 (2019).
[21] F. Niedermann and M. S. Sloth, Phys. Rev. D 103, L041303 (2021).
[22] J. Sakstein and M. Trodden, Phys. Rev. Lett. 124, 161301 (2020).
[23] G. Ye and Y.-S. Piao, Phys. Rev. D 101, 083507 (2020).
[24] M. Zumalacarregui, Phys. Rev. D 102, 023523 (2020).
[25] J. C. Hill, E. McDonough, M. W. Toomey, and S. Alexander, Phys. Rev. D 102, 043507 (2020).
[26] A. Chudaykin, D. Gorbunov, and N. Nedelko, J. Cosmol. Astropart. Phys. 08 (2020) 013.
[27] A. Gogoi, R. K. Sharma, P. Chanda, and S. Das, Astrophys. J. 915, 132 (2021).
[28] M. Braglia, W. T. Emond, F. Finelli, A. E. Gumrukcuoglu, and K. Koyama, Phys. Rev. D 102, 083513 (2020).
[29] F. Niedermann and M. S. Sloth, Phys. Rev. D 102, 063527 (2020).
[30] M. M. Ivanov, E. McDonough, J. C. Hill, M. Simonović, M. W. Toomey, S. Alexander, and M. Zaldarriaga, Phys. Rev. D 102, 103502 (2020).
[31] G. D'Amico, L. Senatore, P. Zhang, and H. Zheng, J. Cosmol. Astropart. Phys. 05 (2021) 072.
[32] G. Ye and Y.-S. Piao, Phys. Rev. D 102, 083523 (2020).
[33] F. Niedermann and M. S. Sloth, Phys. Rev. D 103, 103537 (2021).
[34] R. Murgia, G. F. Abellán, and V. Poulin, Phys. Rev. D 103, 063502 (2021).
[35] T. L. Smith, V. Poulin, J. L. Bernal, K. K. Boddy, M. Kamionkowski, and R. Murgia, Phys. Rev. D 103, 123542 (2021).
[36] A. Chudaykin, D. Gorbunov, and N. Nedelko, Phys. Rev. D 103, 043529 (2021).
[37] M. Carrillo González, Q. Liang, J. Sakstein, and M. Trodden, J. Cosmol. Astropart. Phys. 04 (2021) 063.
[38] V. K. Oikonomou, Phys. Rev. D 103, 044036 (2021).
[39] O. Seto and Y. Toda, Phys. Rev. D 103, 123501 (2021).
[40] S. X. Tian and Z.-H. Zhu, Phys. Rev. D 103, 043518 (2021).
[41] K. Freese and M. W. Winkler, arXiv:2102.13655.
[42] S. Nojiri, S. D. Odintsov, D. Saez-Chillon Gomez, and G. S. Sharov, Phys. Dark Universe 32, 100837 (2021).
[43] S. Vagnozzi, S. Dhawan, M. Gerbino, K. Freese, A. Goobar, and O. Mena, Phys. Rev. D 98, 083501 (2018).
[44] R. C. Nunes, J. Cosmol. Astropart. Phys. 05 (2018) 052.
[45] V. Poulin, K. K. Boddy, S. Bird, and M. Kamionkowski, Phys. Rev. D 97, 123504 (2018).
[46] W. Yang, S. Pan, E. Di Valentino, R. C. Nunes, S. Vagnozzi, and D. F. Mota, J. Cosmol. Astropart. Phys. 09 (2018) 019.
[47] A. Banihashemi, N. Khosravi, and A. H. Shirazi, Phys. Rev. D 101, 123521 (2020).
[48] R.-Y. Guo, J.-F. Zhang, and X. Zhang, J. Cosmol. Astropart. Phys. 02 (2019) 054.
[49] L. L. Graef, M. Benetti, and J. S. Alcaniz, Phys. Rev. D 99, 043519 (2019).
[50] C. D. Kreisch, F.-Y. Cyr-Racine, and O. Doré, Phys. Rev. D 101, 123505 (2020).
[51] K. L. Pandey, T. Karwal, and S. Das, J. Cosmol. Astropart. Phys. 07 (2020) 026.
[52] M. Martinelli, N. B. Hogg, S. Peirone, M. Bruni, and D. Wands, Mon. Not. R. Astron. Soc. 488, 3423 (2019).
[53] K. Vattis, S. M. Koushiappas, and A. Loeb, Phys. Rev. D 99, 121302 (2019).
[54] M.-X. Lin, G. Benevento, W. Hu, and M. Raveri, Phys. Rev. D 100, 063542 (2019).
[55] X. Li and A. Shafieloo, Astrophys. J. Lett. 883, L3 (2019).
[56] E. Di Valentino, R. Z. Ferreira, L. Visinelli, and U. Danielsson, Phys. Dark Universe 26, 100385 (2019).
[57] W. Yang, S. Pan, S. Vagnozzi, E. Di Valentino, D. F. Mota, and S. Capozziello, J. Cosmol. Astropart. Phys. 11 (2019) 044.
[58] S. Pan, W. Yang, E. Di Valentino, E. N. Saridakis, and S. Chakraborty, Phys. Rev. D 100, 103520 (2019).
[59] S. Vagnozzi, Phys. Rev. D 102, 023518 (2020).
[60] L. Visinelli, S. Vagnozzi, and U. Danielsson, Symmetry 11, 1035 (2019).
[61] Y.-F. Cai, M. Khurshudyan, and E. N. Saridakis, Astrophys. J. 888, 62 (2020).
[62] N. Schöneberg, J. Lesgourgues, and D. C. Hooper, J. Cosmol. Astropart. Phys. 10 (2019) 029.
[63] S. Pan, W. Yang, E. Di Valentino, A. Shafieloo, and S. Chakraborty, J. Cosmol. Astropart. Phys. 06 (2020) 062.
[64] E. Di Valentino, A. Melchiorri, O. Mena, and S. Vagnozzi, Phys. Dark Universe 30, 100666 (2020).
[65] J. Solà Peracaula, A. Gomez-Valent, J. de Cruz Pérez, and C. Moreno-Pulido, Astrophys. J. Lett. 886, L6 (2019).
[66] M. Escudero and S. J. Witte, Eur. Phys. J. C 80, 294 (2020).
[67] E. Di Valentino, A. Melchiorri, O. Mena, and S. Vagnozzi, Phys. Rev. D 101, 063502 (2020).
[68] M. Liu, Z. Huang, X. Luo, H. Miao, N. K. Singh, and L. Huang, Sci. China Phys. Mech. Astron. 63, 290405 (2020).
[69] L. Hart and J. Chluba, Mon. Not. R. Astron. Soc. 493, 3255 (2020).
[70] O. Akarsu, J. D. Barrow, L. A. Escamilla, and J. A. Vazquez, Phys. Rev. D 101, 063528 (2020).
[71] D. Benisty, arXiv:1912.11124.
[72] W. Yang, E. Di Valentino, S. Pan, S. Basilakos, and A. Paliathanasis, Phys. Rev. D 102, 063503 (2020).
[73] G. Choi, M. Suzuki, and T. T. Yanagida, Phys. Rev. D 101, 075031 (2020).
[74] M. Lucca and D. C. Hooper, Phys. Rev. D 102, 123502 (2020).
[75] N. B. Hogg, M. Bruni, R. Crittenden, M. Martinelli, and S. Peirone, Phys. Dark Universe 29, 100583 (2020).

[76] G. Benevento, W. Hu, and M. Raveri, Phys. Rev. D **101**, 103517 (2020).
[77] W. E. V. Barker, A. N. Lasenby, M. P. Hobson, and W. J. Handley, Phys. Rev. D **102**, 024048 (2020).
[78] A. Gómez-Valent, V. Pettorino, and L. Amendola, Phys. Rev. D **101**, 123513 (2020).
[79] O. Akarsu, N. Katırcı, S. Kumar, R. C. Nunes, B. Öztürk, and S. Sharma, Eur. Phys. J. C **80**, 1050 (2020).
[80] G. Ballesteros, A. Notari, and F. Rompineve, J. Cosmol. Astropart. Phys. 11 (2020) 024.
[81] B. S. Haridasu and M. Viel, Mon. Not. R. Astron. Soc. **497**, 1757 (2020).
[82] G. Alestas, L. Kazantzidis, and L. Perivolaropoulos, Phys. Rev. D **101**, 123516 (2020).
[83] K. Jedamzik and L. Pogosian, Phys. Rev. Lett. **125**, 181302 (2020).
[84] M. Ballardini, M. Braglia, F. Finelli, D. Paoletti, A. A. Starobinsky, and C. Umiltà, J. Cosmol. Astropart. Phys. 10 (2020) 044.
[85] A. Banerjee, H. Cai, L. Heisenberg, E. O. Colgáin, M. M. Sheikh-Jabbari, and T. Yang, Phys. Rev. D **103**, L081305 (2021).
[86] E. Elizalde, M. Khurshudyan, S. D. Odintsov, and R. Myrzakulov, Phys. Rev. D **102**, 123501 (2020).
[87] M. Gonzalez, M. P. Hertzberg, and F. Rompineve, J. Cosmol. Astropart. Phys. 10 (2020) 028.
[88] S. Capozziello, M. Benetti, and A. D. A. M. Spallicci, Found. Phys. **50**, 893 (2020).
[89] A. Das and S. Ghosh, arXiv:2011.12315.
[90] A. Banihashemi, N. Khosravi, and A. Shafieloo, J. Cosmol. Astropart. Phys. 06 (2021) 003.
[91] S. Roy Choudhury, S. Hannestad, and T. Tram, J. Cosmol. Astropart. Phys. 03 (2021) 084.
[92] T. Brinckmann, J. H. Chang, and M. LoVerde, Phys. Rev. D **104**, 063523 (2021); arXiv:2012.11830.
[93] H. Moshafi, S. Baghram, and N. Khosravi, arXiv:2012.14377.
[94] G. Alestas and L. Perivolaropoulos, Mon. Not. R. Astron. Soc. **504**, 3956 (2021).
[95] F. Beutler, C. Blake, M. Colless, D. H. Jones, L. Staveley-Smith, L. Campbell, Q. Parker, W. Saunders, and F. Watson, Mon. Not. R. Astron. Soc. **416**, 3017 (2011).
[96] A. J. Ross, L. Samushia, C. Howlett, W. J. Percival, A. Burden, and M. Manera, Mon. Not. R. Astron. Soc. **449**, 835 (2015).
[97] J. L. Bernal, L. Verde, and A. G. Riess, J. Cosmol. Astropart. Phys. 10 (2016) 019.
[98] G. E. Addison, D. J. Watts, C. L. Bennett, M. Halpern, G. Hinshaw, and J. L. Weiland, Astrophys. J. **853**, 119 (2018).
[99] P. Lemos, E. Lee, G. Efstathiou, and S. Gratton, Mon. Not. R. Astron. Soc. **483**, 4803 (2019).
[100] K. Aylor, M. Joy, L. Knox, M. Millea, S. Raghunathan, and W. L. K. Wu, Astrophys. J. **874**, 4 (2019).
[101] L. Knox and M. Millea, Phys. Rev. D **101**, 043533 (2020).
[102] N. Arendse *et al.*, Astron. Astrophys. **639**, A57 (2020).
[103] G. Efstathiou, arXiv:2103.08723.
[104] P. Motloch, Phys. Rev. D **101**, 123509 (2020).
[105] M. Chu and L. Knox, Astrophys. J. **620**, 1 (2005).
[106] R. K. Sachs and A. M. Wolfe, Astrophys. J. **147**, 73 (1967).
[107] M. J. Rees and D. W. Sciama, Nature (London) **217**, 511 (1968).
[108] E. Calabrese, A. Slosar, A. Melchiorri, G. F. Smoot, and O. Zahn, Phys. Rev. D **77**, 123531 (2008).
[109] C. Krishnan, E. O. Colgáin, Ruchika, A. A. Sen, M. M. Sheikh-Jabbari, and T. Yang, Phys. Rev. D **102**, 103525 (2020).
[110] K. Jedamzik, L. Pogosian, and G.-B. Zhao, Commun. Phys. **4**, 123 (2021).
[111] W. Lin, X. Chen, and K. J. Mack, arXiv:2102.05701.
[112] M. G. Dainotti, B. De Simone, T. Schiavone, G. Montani, E. Rinaldi, and G. Lambiase, Astrophys. J. **912**, 150 (2021).
[113] C. Krishnan, R. Mohayaee, E. O. Colgáin, M. M. Sheikh-Jabbari, and L. Yin, arXiv:2105.09790.
[114] S. Vagnozzi, F. Pacucci, and A. Loeb, arXiv:2105.10421.
[115] C. Krishnan, R. Mohayaee, E. O. Colgáin, M. M. Sheikh-Jabbari, and L. Yin, arXiv:2106.02532.
[116] C.-P. Ma and E. Bertschinger, Astrophys. J. **455**, 7 (1995).
[117] Z. Hou, R. Keisler, L. Knox, M. Millea, and C. Reichardt, Phys. Rev. D **87**, 083008 (2013).
[118] G. Cabass, M. Gerbino, E. Giusarma, A. Melchiorri, L. Pagano, and L. Salvati, Phys. Rev. D **92**, 063534 (2015).
[119] J. A. Kable, G. E. Addison, and C. L. Bennett, Astrophys. J. **905**, 164 (2020).
[120] G. Efstathiou and S. Gratton, arXiv:1910.00483.
[121] N. Aghanim *et al.* (Planck Collaboration), Astron. Astrophys. **641**, A8 (2020).
[122] N. Aghanim *et al.* (Planck Collaboration), Astron. Astrophys. **641**, A5 (2020).
[123] S. Alam *et al.* (BOSS Collaboration), Mon. Not. R. Astron. Soc. **470**, 2617 (2017).
[124] A. Lewis, A. Challinor, and A. Lasenby, Astrophys. J. **538**, 473 (2000).
[125] A. Lewis and S. Bridle, Phys. Rev. D **66**, 103511 (2002).
[126] A. Gelman and D. B. Rubin, Stat. Sci. **7**, 457 (1992).
[127] S. Vagnozzi, arXiv:1907.08010.
[128] C.-G. Park and B. Ratra, Astrophys. J. **882**, 158 (2019).
[129] W. Handley, Phys. Rev. D **103**, L041301 (2021).
[130] E. Di Valentino, A. Melchiorri, and J. Silk, Nat. Astron. **4**, 196 (2020).
[131] G. Efstathiou and S. Gratton, Mon. Not. R. Astron. Soc. **496**, L91 (2020).
[132] E. Di Valentino, A. Melchiorri, and J. Silk, Astrophys. J. Lett. **908**, L9 (2021).
[133] E. Di Valentino, S. Gariazzo, O. Mena, and S. Vagnozzi, J. Cosmol. Astropart. Phys. 07 (2020) 045.
[134] E. Di Valentino *et al.*, Astropart. Phys. **131**, 102607 (2021).
[135] S. Vagnozzi, E. Di Valentino, S. Gariazzo, A. Melchiorri, O. Mena, and J. Silk, Phys. Dark Universe **33**, 100851 (2021).
[136] E. Di Valentino, A. Melchiorri, O. Mena, S. Pan, and W. Yang, Mon. Not. R. Astron. Soc. **502**, L23 (2021).
[137] S. Vagnozzi, A. Loeb, and M. Moresco, Astrophys. J. **908**, 84 (2021).
[138] S. Cao, J. Ryan, and B. Ratra, Mon. Not. R. Astron. Soc. **504**, 300 (2021).
[139] S. Dhawan, J. Alsing, and S. Vagnozzi, Mon. Not. R. Astron. Soc. **506**, L1 (2021).

[140] J. E. Gonzalez, M. Benetti, R. von Marttens, and J. Alcaniz, arXiv:2104.13455.
[141] G. Cabass, E. Di Valentino, A. Melchiorri, E. Pajer, and J. Silk, Phys. Rev. D **94**, 023523 (2016).
[142] G. E. Addison, Y. Huang, D. J. Watts, C. L. Bennett, M. Halpern, G. Hinshaw, and J. L. Weiland, Astrophys. J. **818**, 132 (2016).
[143] S. Galli, K. Benabed, F. Bouchet, J.-F. Cardoso, F. Elsner, E. Hivon, A. Mangilli, S. Prunet, and B. Wandelt, Phys. Rev. D **90**, 063504 (2014).
[144] P. Ade *et al.* (Simons Observatory Collaboration), J. Cosmol. Astropart. Phys. 02 (2019) 056.
[145] K. N. Abazajian *et al.* (CMB-S4 Collaboration), arXiv: 1610.02743.
[146] P. Svrcek and E. Witten, J. High Energy Phys. 06 (2006) 051.
[147] A. Arvanitaki, S. Dimopoulos, S. Dubovsky, N. Kaloper, and J. March-Russell, Phys. Rev. D **81**, 123530 (2010).
[148] M. Kamionkowski, J. Pradler, and D. G. E. Walker, Phys. Rev. Lett. **113**, 251302 (2014).
[149] T. Karwal and M. Kamionkowski, Phys. Rev. D **94**, 103523 (2016).
[150] L. Visinelli and S. Vagnozzi, Phys. Rev. D **99**, 063517 (2019).
[151] T. Rudelius, J. Cosmol. Astropart. Phys. 09 (2015) 020.
[152] M. Montero, A. M. Uranga, and I. Valenzuela, J. High Energy Phys. 08 (2015) 032.
[153] D. Blas, J. Lesgourgues, and T. Tram, J. Cosmol. Astropart. Phys. 07 (2011) 034.
[154] S. Ho, C. Hirata, N. Padmanabhan, U. Seljak, and N. Bahcall, Phys. Rev. D **78**, 043519 (2008).
[155] T. Giannantonio and W. J. Percival, Mon. Not. R. Astron. Soc. **441**, L16 (2014).
[156] J. Renk, M. Zumalacarregui, and F. Montanari, J. Cosmol. Astropart. Phys. 07 (2016) 040.
[157] E. Giusarma, S. Vagnozzi, S. Ho, S. Ferraro, K. Freese, R. Kamen-Rubio, and K.-B. Luk, Phys. Rev. D **98**, 123526 (2018).
[158] S. Vagnozzi, L. Visinelli, O. Mena, and D. F. Mota, Mon. Not. R. Astron. Soc. **493**, 1139 (2020).
[159] S. Dodelson, *Modern Cosmology* (Academic Press, Amsterdam, 2003).
[160] R. C. Nunes and S. Vagnozzi, Mon. Not. R. Astron. Soc. **505**, 5427 (2021).
[161] M. Escudero and S. J. Witte, Eur. Phys. J. C **81**, 515 (2021).
[162] L. Lombriser, Phys. Lett. B **803**, 135303 (2020).
[163] H. Desmond, B. Jain, and J. Sakstein, Phys. Rev. D **100**, 043537 (2019); **101**, 069904(E) (2020); **101**, 129901(E) (2020).
[164] Q. Ding, T. Nakama, and Y. Wang, Sci. China Phys. Mech. Astron. **63**, 290403 (2020).
[165] H. Desmond and J. Sakstein, Phys. Rev. D **102**, 023007 (2020).
[166] G. Alestas, L. Kazantzidis, and L. Perivolaropoulos, Phys. Rev. D **103**, 083517 (2021).
[167] R.-G. Cai, Z.-K. Guo, L. Li, S.-J. Wang, and W.-W. Yu, Phys. Rev. D **103**, L121302 (2021).
[168] V. Marra and L. Perivolaropoulos, Phys. Rev. D **104**, L021303 (2021).
[169] G. Efstathiou, arXiv:2007.10716.
[170] E. Mortsell, A. Goobar, J. Johansson, and S. Dhawan, arXiv:2105.11461.
[171] E. Mortsell, A. Goobar, J. Johansson, and S. Dhawan, arXiv:2106.09400.
[172] M. H. Abitbol *et al.* (Simons Observatory Collaboration), Bull. Am. Astron. Soc. **51**, 147 (2019); arXiv:1907.08284.
[173] See http://www.hpc.cam.ac.uk.
[174] See http://www.dirac.ac.uk.